Stabilization of unilamellar catanionic vesicles induced by β-cyclodextrins: A strategy for a tunable drug delivery depot

Gesmi Milcovich[a], Filipe E. Antunes[b], Mario Grassi[c,*], Fioretta Asaro[a]

[a] Department of Chemical and Pharmaceutical Sciences, University of Trieste, via L. Giorgieri 1, 34127 Trieste, Italy
[b] Coimbra Chemistry Centre, Dept. of Chemistry, University of Coimbra, Rua Larga, Coimbra, Portugal
[c] Department of Engineering and Architecture, University of Trieste, via A. Valerio 6/A, 34127 Trieste, Italy

ARTICLE INFO

Keywords:
Catanionic vesicles
Cyclodextrin
Diffusion
NMR
Self-assembly

ABSTRACT

The limited stability of catanionic vesicles has discouraged their wide use for encapsulation and controlled release of active substances. Their structure can easily break down to form lamellar phases, micelles or rearrange into multilamellar vesicles, as a consequence of small changes in their composition. However, despite the limited stability, catanionic vesicles possess an attractive architecture, which is able to efficiently encapsulate both hydrophobic and hydrophilic molecules. Therefore, improving the stability of the vesicles, as well as the control on unilamellar structures, are prerequisites for their wider application range. This study focuses on the impact of β-cyclodextrins for the stabilization of SDS/CTAB catanionic vesicles. Molar ratio and sample preparation procedures have been investigated to evaluate the temperature stability of catanionic vesicles. Diffusion and spectroscopic techniques evidenced that when β-cyclodextrins are added, unilamellar structures are stabilized above the multilamellar-unilamellar vesicles critical temperature. The results evidence encouraging perspectives for the use of vesicular nanoreservoirs for drug depot applications.

1. Introduction

Catanionic vesicles are self-assembled nanostructures composed of dilute mixtures of oppositely charged surfactants. They have emerged in the last twenty years as a relevant and exciting new type of vesicle systems (Antunes et al., 2004, 2009; Kaler et al., 1992; Marques et al., 1993; Medronho et al., 2006; Milcovich et al., 2016, 2017; dos Santos et al., 2013). They are usually spherical, their polydispersity can vary remarkably and they can experience either monolayer or multilayer architectures. The advantage of using such nanoresevoirs in drug delivery relies on their elegant ability to compartmentalize both hydrophobic and hydrophilic molecules.

Cyclodextrins (CD) are cyclic oligosaccharides composed by glucose units connected through (1,4)-α-glucoside bonds (Szejtli, 1998). Their 3D molecular structure resembles a truncated cone, with a polar exterior and a less polar inner core (Connors, 1997). Cyclodextrins are able to generate inclusion complexes in aqueous solution by replacing water molecules in their cavity with small hydrophobic molecules or hydrophobic moieties of bigger molecules, and thus changing their solubility. They are mainly produced by starch enzymatic degradation, employing cyclodextrin glycosyl transferases (Biwer et al., 2002). So far, these cyclic oligosaccharides exhibit several industrial applications for pharmaceutical formulations, food products and cosmetics (Davis and Brewster, 2004; Hegdes, 1998). The constant and extensive interest on β-cyclodextrin for pharmaceutical and biomedical applications relies on their approval for human use (Li and Loh, 2008).

They also demonstrated to be able to modulate the rheology properties of hydrophobically modified polymers (Karlson et al., 2002). Depending on their number of glucose units, cyclodextrins can be classified according to Table 1.

An interesting feature of cyclodextrins concerns their aqueous solubility, which is influenced by the number of glucose units. The extremely low water solubility of β-cyclodextrin, compared to α and γ-cyclodextrin, is due to the high energy H-bond network between the C2 and C3 hydroxyl groups (Szejtli, 1998). Nevertheless, this low solubility is adequate for improving the solubility of the poorly soluble included guests (Tewes et al., 2008; Thi et al., 2009).

Several techniques are described in the literature to study the inclusion of the hydrophobic tail of a surfactant into a cyclodextrin cavity, like NMR (Cabaleiro-Lago et al., 2005; Sehgal et al., 2006), calorimetry (De Lisi et al., 2003), neutron scattering (Alami et al., 2002), sound measurements (Junquera et al., 1993), capillary electrophoresis (Bendazzoli et al., 2010), surface tension (Bai et al., 2008) and conductivity (Junquera et al., 1997; Mehta et al., 2008; Sehgal et al.,

* Corresponding author.
E-mail address: mario.grassi@dia.units.it (M. Grassi).

Accepted 6 July 2018

Table 1
Characteristics of cyclodextrins (Connors, 1997; Del Valle, 2004).

Specie	Number of glucose units	Outer diameter	Inner diameter	Height	Solubility
α-cyclodextrin	6	1.46 nm	0.52 nm	0.8 nm	0.1211 M
β-cyclodextrin	7	1.54 nm	0.66 nm	0.8 nm	0.0163 M
γ-cyclodextrin	8	1.75 nm	0.84 nm	0.8 nm	0.1680 M

2006). β-Cyclodextrins are characterized by a high binding constant toward surfactants (host-guest complexes) (Valente and Söderman, 2014) and the formation of the mentioned complexes competes with surfactant micellization. β-Cyclodextrin was found to form inclusion complexes with the surfactants studied herein for the preparation of catanionic vesicles. Their binding constants are listed below:

- cetyl-trimethyl ammonium bromide (CTAB) with β-cyclodextrin: $5 \cdot 10^4\,M^{-1}$ (Cabaleiro-Lago et al., 2005);
- sodium dodecyl-sulfate (SDS) with β-cyclodextrin: $500\,M^{-1}$ (Junquera et al., 1993).

Thus, the presence of cyclodextrin can shift the surfactant CMC (critical micellar concentration) to higher concentrations, in a cyclodextrin-concentration dependent manner (Jiang et al., 2003). Moreover, β-cyclodextrin can interact also with surfactants (see Fig. 1), which composes vesicular aggregates, thus modulating vesicles properties (Yan et al., 2011).

The aim of this study is to understand such interactions, focusing on the influence of molar ratio, sample preparation procedure (i.e. addition of β-cyclodextrin before or after vesicles are generated) and temperature range on the stability of β-cyclodextrin doped catanionic vesicles. We hypothesize that the presence of β-cyclodextrin on catanionic vesicles can lead to an *in situ* stabilizing effect toward multi-to-unilamellar transition of catanionic vesicles, due to their complexation/binding features on the catanionic vesicle components (Fig. 2).

2. Materials and methods

2.1. Materials and sample preparation

Sodium dodecyl-sulfate (SDS) has been obtained from BDH Chemicals Ltd. Pool. England (purity grade 99,0%), while cetyl-trimethyl ammonium bromide (CTAB) has been purchased from Sigma-Aldrich (puriss ≥ 96%). Aqueous solutions of CTAB and SDS have been prepared and subsequently mixed in order to obtain vesicular solutions. Different molar ratios (R, according to equation (1)) have been employed, at a constant concentration of C = 6 mM (i.e. about 0.2% wt).

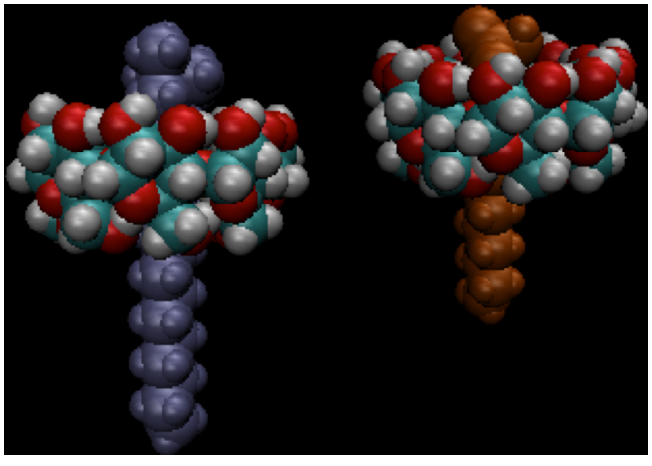

Fig. 1. Schematic representation of surfactant-cyclodextrin binding (Humphrey et al., 1996; Loftsson and Brewster, 1996).

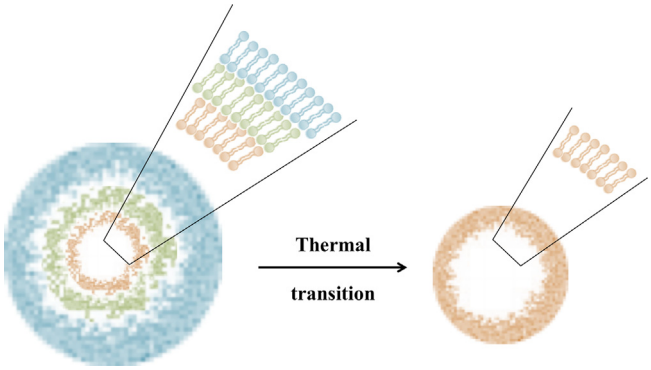

Fig. 2. Schematic model of the catanionic vesicles multi-to-unilamellar transition: the vesicles inner pool is represented as the empty core of the vesicular spherules (Andreozzi et al., 2010; Milcovich and Asaro, 2012).

$$R = \frac{[SDS]}{[CTAB]} \tag{1}$$

β-Cyclodextrin (kindly provided from Vectorpharma Spa) was used in a fixed concentration of 1 mM.

The preparation of β-cyclodextrin-vesicles systems by the addition of β-cyclodextrin to the pre-formed vesicles will be referred to "standard preparation", while the addition of β-cyclodextrin to surfactant monomeric solutions will be referred to "alternative preparation".

2.2. Multinuclear NMR experiments

^{1}H NMR measurements were carried out on a Jeol Eclipse 400 NMR spectrometer (9.4 T), equipped with a Jeol NM-EVTS3 variable temperature unit, operating at 400 MHz for ^{1}H, with lock on $CDCl_3$, in coaxial tube. ^{23}Na NMR measurements (Woessner, 2001) were carried out on a Jeol Eclipse 400 NMR spectrometer (9.4 T), equipped with a Jeol NM-EVTS3 variable temperature unit, operating at 105.75 MHz, without field frequency lock. The ^{23}Na-R_2 (transverse relaxation rate $R_2 = 1/T_2$) were measured by Hahn Echo.

2.3. PGSTE (Pulsed-gradient stimulated-echo) measurements

The ^{1}H NMR measurements were carried out on a Varian 500 MHz NMR spectrometer (11.74 T) operating at 500 MHz for ^{1}H, equipped with a model L650 Highland Technology pulsed field gradient (PFA) amplifier (10 A) and a standard 5 mm indirect detection, PFG probe. The lock was made on $CDCl_3$ in coaxial tube, containing tetramethylsilane (TMS) as ^{1}H chemical shift reference. A oneshot sequence has been employed for diffusion measurements (Johnson, 1999; Pelta et al., 2002), with 20 different z-gradient strengths, Gz, between 0.02 and 0.54 T/m, a pulsed gradient duration, δ, of 2 ms, and at different diffusion interval (Δ). At each gradient strength, 64 transients have been accumulated employing a spectral width of 11 ppm over 16 k data points. Solvent suppression was accomplished by presaturation. Gradients were calibrated on the value of $D = 1.90 \cdot 10^{-9}\,m^2\,s^{-1}$ for ^{1}H in D_2O (99.9%) at 25 °C (Antalek, 2002). The values of the self-diffusion coefficient, D, were obtained by Tanner equation fitting to experimental data (Tanner, 1970) (Eq. (2)),

$$\frac{E}{E_0} = \exp(-bD) \quad b = (\gamma\delta G)^2 \cdot \left(\Delta - \frac{\delta}{3}\right) \tag{2}$$

where:

- E and E_0 are the signal intensities in the presence and absence of Gz, respectively,

– D is the diffusion coefficient,
– γ is the nuclear gyromagnetic ratio $26.75 \cdot 10^7$ rad s^{-1} T^{-1} for ^1H nucleus,
– δ is the gradient pulse width,
– G is the gradient amplitude,
– (Δ-δ/3) correspond to the diffusion time corrected for the effects of finite gradient pulse.

PGSTE NMR spectra were processed using MestRenova and self-diffusion coefficients were determined by linear regression with Excel.

2.4. UV–Vis (Turbidity) measurements

Spectral and absorbance measurements were carried out by using Shimadzu UV/Vis spectrophotometer model UV-2450, equipped with a Peltier temperature control unit; 1.0 cm thickness matched quartz cells were used for the entire experimental work.

2.5. Polarized light microscopy

A Leitz Pol-Orthoplan microscope, equipped with differential interference contrast (DIC) lenses, was used. The main goal was to check the presence of crystals or anisotropic liquid crystals, such as lamellar phases, under polarized light. Samples were observed at room temperature, both immediately after preparation and several days later.

2.6. Dynamic light scattering (DLS)

The mean particle diameter of the aggregates and polydispersion index were determined by dynamic light scattering (photon correlation spectroscopy, PCS) using an N5 Particle Analyzer (Beckman Coulter Inc., USA), equipped with a Peltier temperature control unit. Data were collected at 90° scattering angle. The time-averaged autocorrelation functions were transformed into intensity-weighted distributions of the apparent hydrodynamic diameter using the available Beckman PCS software. The average values of size were calculated with the data obtained from three measurements ± SD.

3. Results and discussion

3.1. System characterization

A minimum SDS/CTAB molar ratio of R = 1.6 was found to be required in order to avoid precipitation/flocculates. High molar ratio values (R > 2.6) evidenced the co-existence of micelles that can disturb vesicle investigation and observation (Andreozzi et al., 2010). A SDS/CTAB molar ratio of R = 1.85 was investigated, as it ensures the appropriate stability (see Supplementary, Fig. S1).

Supplementary Figs. S1–S4 associated with this article can be found, in the online version, at https://doi.org/10.1016/j.ijpharm.2018.07.026.

^1H NMR was performed and β-cyclodextrin peaks have been assigned (see Supplementary, Fig. S2). ^1H NMR cannot directly detect vesicle signals, due to their large dimension and high relaxation range. On the other hand, the exchanging surfactants and cyclodextrins can be detected, as per Fig. 3. CTAB is completely embedded in the vesicular aggregates, according to the ^1H NMR, where no CTAB signal is detected (see Supplementary, Fig. S3).

Despite the addition of β-cyclodextrin, solutions remain isotropic, as no liquid crystals were present in any sample, according to polarized light microscopy (data not shown). PGSTE results confirmed those findings, with no shifts in the diffusion coefficient and only a single diffusion coefficient D detected for β-cyclodextrin signals.

The present system shows the SDS excess throughout vesicle composition. SDS molecules are in exchange between vesicles and bulk solution, as demonstrated by PGSTE NMR diffusion measurements, with a quite lower exchange rate than a micellar system (Fig. 4).

The diffusion coefficients *D* were measured and it was possible to assess that β-cyclodextrin is not entrapped in the aqueous inner pool of vesicles, as otherwise β-cyclodextrin *D* was expected to be extremely low, compared to a simple β-cyclodextrin water solution (Morris and Johnson, 1993) (see Supplementary, Fig. S4).

According to Table 2, β-cyclodextrin detectable signals correspond to a constant D coefficient: thus, β-cyclodextrin diffusion is not influenced by the presence of vesicular aggregates.

Further analysis demonstrate that monomeric dodecylsulfate in water possesses a coefficient $D = 6.2 \cdot 10^{-10}$ m^2/s. Thus, dodecylsulfate

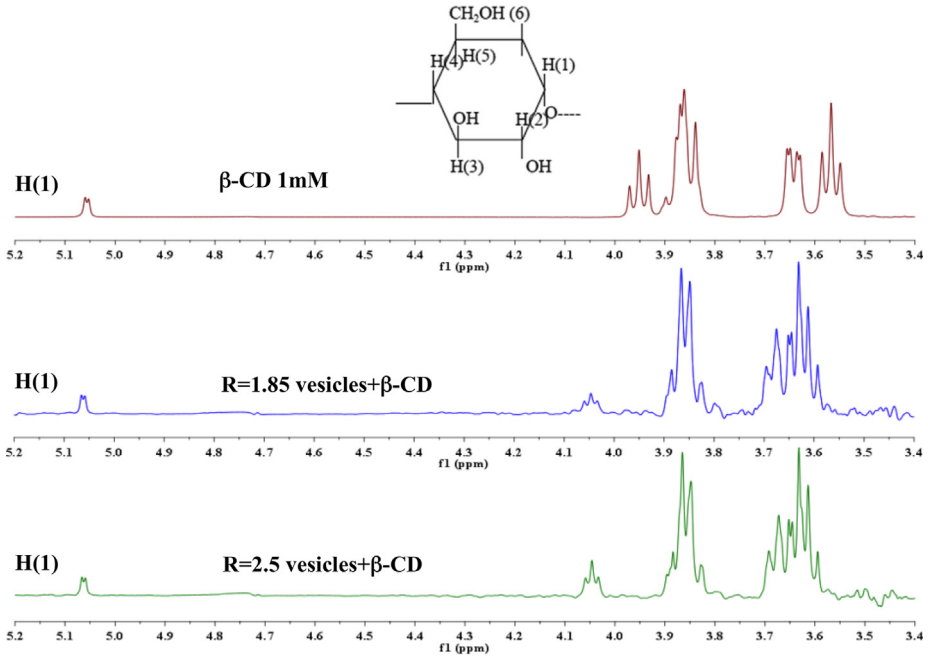

Fig. 3. Comparison of ^1H NMR spectra in water, all referred to TMS peak.

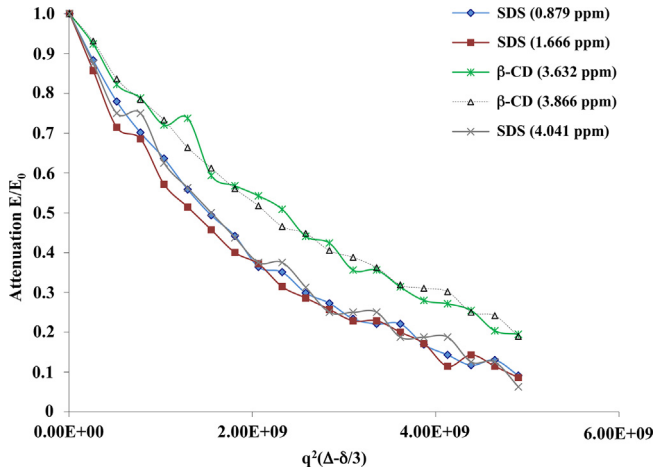

Fig. 4. Plot of the echo decays (only detectable signals) at 30 °C (Δ = 60 ms) for R = 1.85 vesicles with β-cyclodextrin.

Table 2
Diffusion coefficients of β-cyclodextrin doped vesicles (excess surfactant SDS and βcyclodextrin diffusion coefficients are reported).

Sample	SDS	β-cyclodextrin
SDS + βCD	$5.5 \cdot 10^{-10}$ m²/s	$3.1 \cdot 10^{-10}$ m²/s
Vesicles + βCD, R = 1.85 ("alternative")	$4.2 \cdot 10^{-10}$ m²/s	$3.1 \cdot 10^{-10}$ m²/s
Vesicles + βCD, R = 1.85	$4.7 \cdot 10^{-10}$ m²/s	$3.1 \cdot 10^{-10}$ m²/s

exhibits a remarkable decrease in terms of diffusion, which might be related to a dynamic complexation with β-cyclodextrin.

3.2. *In situ stabilization of catanionic vesicles by β-cyclodextrins*

When prepared, vesicle dispersion appears milky, but the turbidity dramatically decreases by heating. This is related to a multi-to-unilamellar transition together with a decrease of the vesicle size, as reported in literature (Andreozzi et al., 2010). This phenomenon is anticipated by sodium dissociation, as per ^{23}Na NMR transverse relaxation rates (R2), and it involves an uptake of free dodecylsulfate into aggregates, as revealed by ^{1}H NMR. Accordingly, ^{23}Na transverse relaxation rates show that Na^+ dissociation anticipates the thermal transition (Milcovich and Asaro, 2012).

The addition of β-cyclodextrins leads to an increase of the critical transition temperature, Tc, and to lower ^{23}Na-R_2 trends. This is supported by the reduction of free dodecylsulfate in the bulk, due to its complexation with β-cyclodextrin.

Moreover, vesicular aggregates do not allow β-cyclodextrin to permeate the bilayer, as shown by PGSTE NMR measurements. The decrease in turbidity is anticipated by a sodium dissociation; this trend is evident in β-cyclodextrin doped samples as well.

Specifically, for what concerns the shift in the critical transition temperature, Tc, normal vesicles usually hold a Tc = 47 °C, while for β-cyclodextrin doped vesicles values around 49–50 °C have been detected. Therefore β-cyclodextrins addition is able to expand the temperature range for multilamellar vesicle, reporting a higher Tc. Viceversa, above the Tc, β-cyclodextrins interaction leads to unilamellar vesicles with higher stability.

The critical temperature (Tc) depends on molar ratio R: lower Tc values correspond to higher molar ratios, R. Thus, it is proposed that ^{23}Na-R_2 trends are related to vesicular dimension and dodecylsulfate amount inside the aggregates (Fig. 5).

Lower R values show higher amounts of free Na^+, probably due to a complexation of dodecylsulfate with β-cyclodextrin, which seems not to participate in aggregates, as inferred by previous ^{1}H NMR integral analyses.

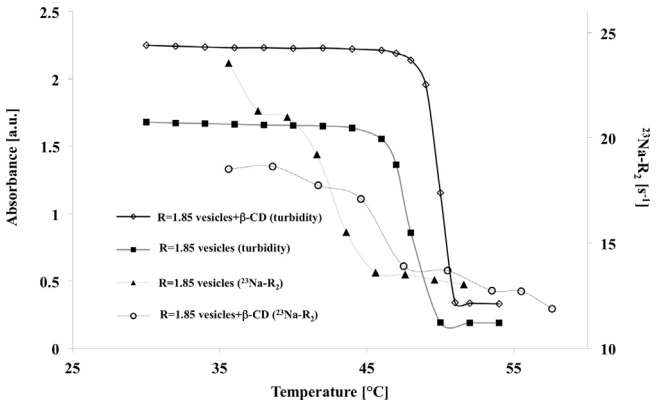

Fig. 5. Effect of β-cyclodextrin addition on turbidity and ^{23}Na-R_2 trends vs. temperature.

^{23}Na transverse relaxation rates evidence that the preparation procedure can influence very much the Na^+ dissociation, as evidenced in Fig. 6. Thus, even though the thermal transition leads to a single final

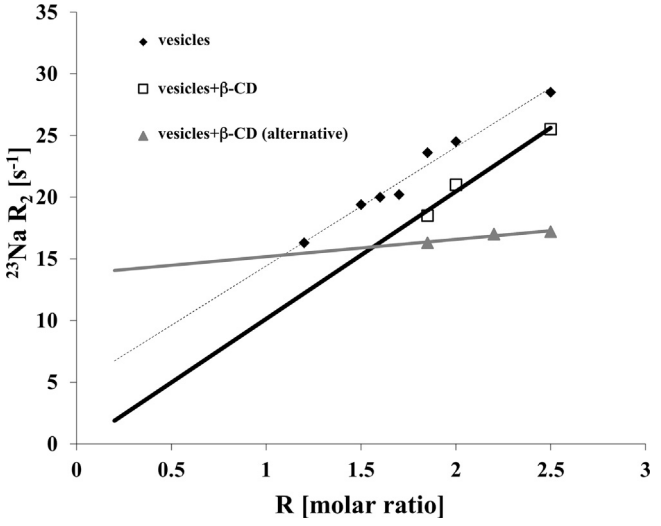

Fig. 6. ^{23}Na-R_2 trends vs. molar ratio before thermal transition, with β-cyclodextrin (both preparation procedures) and without.

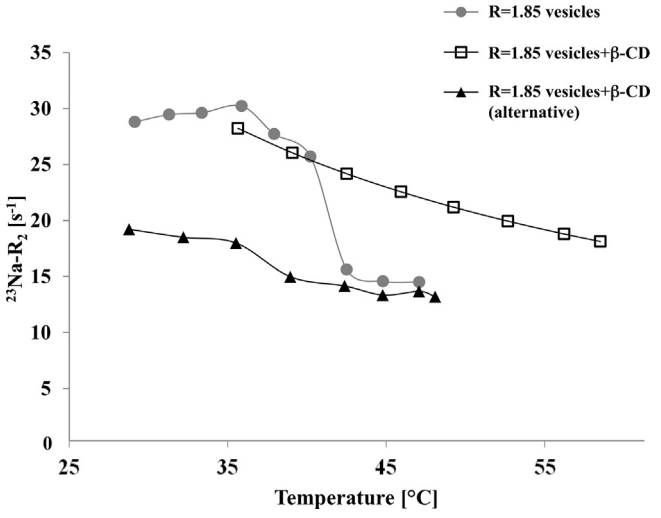

Fig. 7. ^{23}Na-R_2 rates, for samples of vesicles R = 1.85 with β-cyclodextrin ("standard" and "alternative" preparation), compared with simple vesicles.

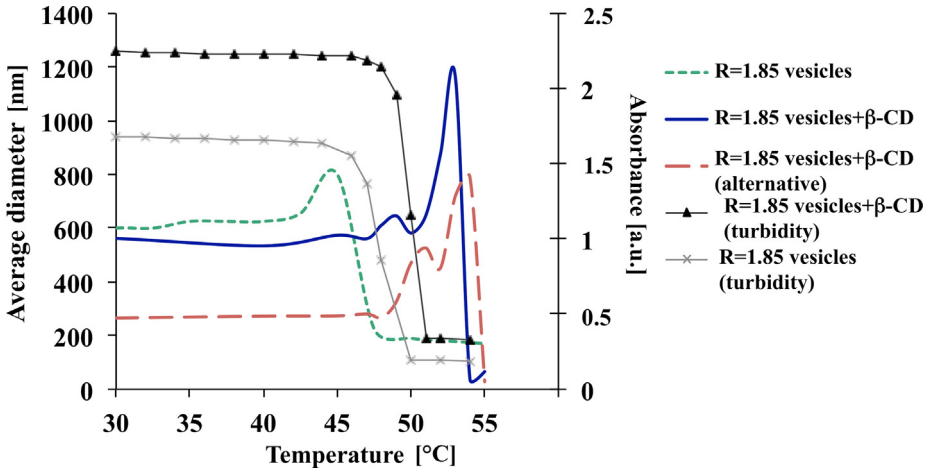

Fig. 8. DLS and turbidity (λ = 550 nm) vs. temperature for vesicles and β-cyclodextrin doped vesicles (both preparations).

R_2, the addition of β-cyclodextrin to monomeric starting solutions enhances the Na^+ dissociation at the early stage.

The "alternative preparation" is supposed to influence remarkably the structural features of the system: ^{23}Na-R_2 values exhibit a linear dependence on R, with the same slope for both simple vesicles and β-cyclodextrin doped vesicles ("standard preparation"). Moreover, the preparation protocol plays a key role in terms of stability of the overall system. Indeed, the ^{23}Na-R_2 trends after the thermal transition reveal that the "standard" fabrication protocol has a stabilization effect on the free Na^+ exchange between the vesicles and the bulk (see Fig. 7), leading to a more easily tunable control toward the vesicle architecture.

These findings allow to determine that the production method referred as "standard" followed by a first thermal transition cycle, leads to stable unilamellar vesicles.

In terms of DLS assessment, when a particle is relatively small and can undergo random thermal (Brownian) motion, time-dependent fluctuations occur and the distance among particles is therefore constantly changing. Constructive and destructive interference of the scattered light by neighboring particles gives rise to the intensity fluctuation at the detector plane. When the particles are extremely small, compared with the light wavelength, the intensity of the scattered light is uniform in all directions (Rayleigh scattering); whereas for larger particles (diameter ≥ 250 nm), the intensity is angle-dependent (Mie scattering).

The size, shape and molecular interactions in the vesicular samples determine frequency shifts, polarization and intensity of the scattered light. Thus, matching DLS characteristics with the other results, allows to gain information about the structure and molecular dynamics of the scattering sample.

DLS analysis (Fig. 8) evidences the presence of a sort of pre-transition, which anticipates the real thermal transition. The results show remarkable differences between the thermal behavior of normal vesicles and β-cyclodextrin doped vesicles. β-Cyclodextrin doped aggregates are also susceptible to a further transition, leading, after the thermal ramp, to quite small aggregates.

As a consequence, the preparation conditions have a major influence on both the size and the thermal behavior of the aggregates, as confirmed by spectroscopic techniques.

4. Conclusions

The results confirm the stabilization of vesicles induced by β-cyclodextrin. PGSTE experiments show an increase of dodecylsulfate in the bulk, mainly in a complexed form together with β-cyclodextrin, as confirmed by ^{23}Na-R_2 trends (decrease of sodium dissociation).

All available CTAB molecules are participating in the vesicle formation, as no CTAB signals were detected (vesicle ^{1}H NMR signals cannot be directly detected, due to very high relaxations). These findings demonstrate that, despite their 'soft' nature, catanionic vesicles can successfully resist to the addition of saccharide-based molecules, such as β-cyclodextrins, leading to an *in situ* vesicular nanoreservoirs stabilization. Indeed, the increase in multi-to-unilamellar transition temperature Tc determines the availability of a broader temperature range for multilamellar vesicles handling and application.

Conversely, above the transition temperature Tc, the addition of β-cyclodextrins elicits the formation of smaller unilamellar vesicles, with higher stability. Overall, depending on the characteristics of the bioactive molecule to be delivered, it is possible to tune the most suitable vesicles size, lamellar composition and temperature range. Thus, such system looks promising for future application in drug delivery, e.g. to decrease bioactive molecules cytotoxicity, enhance small molecules solubility, boosting the absorption of aerosolized bioactive molecules and/or proposes as innovative topical drug delivery solutions.

Acknowledgements

Fondazione CRTrieste is gratefully acknowledged for the purchase of the Varian 500 NMR spectrometer, while University of Trieste (FRA2009) and Italian Ministry of Education (PRIN 2010-11 (20109PLMH2)) are gratefully acknowledged for financial support. The authors wish to thank Ms Sonia Fiuza for editorial assistance.

References

Andreozzi, P., Funari, S.S., La Mesa, C., Mariani, P., Ortore, M.G., Sinibaldi, R., Spinozzi, F., 2010. Multi-to unilamellar transitions in catanionic vesicles. J. Phys. Chem. B 114, 8056–8060.

Alami, E., Abrahmsen-Alami, S., Eastoe, J., Grillo, I., Heenan, R.K., 2002. Interactions between a nonionic gemini surfactant and cyclodextrins investigated by small-angle neutron scattering. J. Colloid Interface Sci. 255, 403–409.

Antalek, B., 2002. Using pulsed gradient spin echo NMR for chemical mixture analysis: How to obtain optimum results. Concepts Magn. Reson. Part A 14, 225–258.

Antunes, F.E., Marques, E.F., Gomes, R., Thuresson, K., Lindman, B., Miguel, M.G., 2004. Network formation of catanionic vesicles and oppositely charged polyelectrolytes. Effect of polymer charge density and hydrophobic modification. Langmuir 20, 4647–4656.

Antunes, F.E., Marques, E.F., Miguel, M.G., Lindman, B., 2009. Polymer-vesicle association. Adv. Colloid Interface Sci. 147–148, 18–35.

Bai, Y., Xu, G.Y., Xin, X., Sun, H.Y., Zhang, H.X., Hao, A.Y., Yang, X.D., Yao, L., 2008. Interaction between cetyltrimethylammonium bromide and cyclodextrin: surface tension and interfacial dilational viscoelasticity studies. Colloid Polym. Sci. 286, 1475–1484.

Bendazzoli, C., Mileo, E., Lucarini, M., Olmo, S., Cavrini, V., Gotti, R., 2010. Capillary electrophoretic study on the interaction between sodium dodecyl sulfate and neutral cyclodextrins. Microchim. Acta 171, 23–31.

Biwer, A., Antranikian, G., Heinzle, E., 2002. Enzymatic production of cyclodextrins. Appl. Microbiol. Biotechnol. 59, 609–617.

Cabaleiro-Lago, C., Nilsson, M., Soderman, O., 2005. Self-diffusion NMR studies of the

host-guest interaction between beta-cyclodextrin and alkyltrimethylammonium bromide surfactants. Langmuir 21, 11637–11644.
Connors, K.A., 1997. The stability of cyclodextrin complexes in solution. Chem. Rev. 97, 1325–1357.
Davis, M.E., Brewster, M.E., 2004. Cyclodextrin-based pharmaceutics: past, present and future. Nat. Rev. Drug Discov. 3, 1023–1035.
De Lisi, R., Lazzara, G., Milioto, S., Muratore, N., Terekhova, I.V., 2003. Characterization of the Cyclodextrin – Surfactant interactions by volume and enthalpy. Langmuir 19, 7188–7195.
Del Valle, E.M.M., 2004. Cyclodextrins and their uses: a review. Process Biochem. 39 (9), 1033–1046.
Hegdes, V., 1998. Industrial applications of cyclodextrins. Chem. Rev. 98, 2035–2044.
Humphrey, W., Dalke, A., Schulten, K., 1996. VMD – visual molecular dynamics. J. Mol. Graph. 14 (1), 33–38.
Jiang, B.-Y., Du, J., Cheng, S.-Q., Pan, J.-W., Zeng, X.-C., Liu, Y.-J., Shunzo, Y., Yoshimi, S., 2003. Effects of cyclodextrins as additives on surfactant CMC. J. Dispers. Sci. Technol. 24 (1), 63–66.
Johnson Jr, C.S., 1999. Diffusion ordered nuclear magnetic resonance spectroscopy: principles and applications. Progr. Nucl. Magn. Reson. Spettrosc. 34, 203–256.
Junquera, E., Tardajos, G., Aicart, E., 1993. Effect of the presence of. beta.-cyclodextrin on the micellization process of sodium dodecyl sulfate or sodium perfluorooctanoate in water. Langmuir 9, 1213–1219.
Junquera, E., Pena, L., Aicart, E., 1997. A Conductimetric study of the interaction of.beta.-cyclodextrin or hydroxypropyl-.beta.-cyclodextrin with dodecyltrimethylammonium bromide in water solution. Langmuir 13, 219–224.
Kaler, E.W., Herrington, K.L., Murthy, A.K., Zasadzinski, J.A.N., 1992. Phase behavior and structures of mixtures of anionic and cationic surfactants. J. Phys. Chem. 96, 6698–6707.
Karlson, L., Thuresson, K., Lindman, B., 2002. A rheological investigation of the complex formation between hydrophobically modified ethyl (hydroxy ethyl) cellulose and cyclodextrin. Carbohyd. Polym. 50, 219–226.
Li, J., Loh, X.J., 2008. Cyclodextrin-based supramolecular architectures: syntheses, structures, and applications for drug and gene delivery. Adv. Drug Deliv. Rev. 60 (9), 1000–1017.
Loftsson, T., Brewster, M.E., 1996. Pharmaceutical applications of cyclodextrins. 1. Drug solubilization and stabilization. J. Pharm. Sci. 85 (10), 1017–1025.
Marques, E., Khan, A., Miguel, M.G., Lindman, B., 1993. Self-assembly in mixtures of a cationic and an anionic surfactant: the sodium dodecyl sulfate-didodecyldimethylammonium bromide-water system. J. Phys. Chem. 97, 4729–4736.
Mehta, S.K., Bhasin, K.K., Dham, S., Singla, M.L., 2008. Micellar behavior of aqueous solutions of dodecyldimethylethylammonium bromide, dodecyltrimethylammonium chloride and tetradecyltrimethylammonium chloride in the presence of α-, β-, HPβ- and γ-cyclodextrins. J. Colloid Interface Sci. 321, 442–451.
Milcovich, G., Asaro, F., 2012. Insights into catanionic vesicles thermal transition by NMR spectroscopy. Progr. Coll. Polym. Sci. 139, 35–38.
Milcovich, G., Antunes, F., Golob, S., Farra, R., Grassi, M., Voinovich, D., Grassi, G., Asaro, F., 2016. Thermo-responsive hydrogels from cellulose-based polyelectrolytes and catanionic vesicles for biomedical application. J. Biomed. Mater. Res. A 104 (7), 1668–1679.
Milcovich, G., Lettieri, S., Antunes, F.E., Medronho, B., Fonseca, A.C., Coelho, J.F.J., Marizza, P., Perrone, F., Farra, R., Dapas, B., Grassi, G., Grassi, M., Giordani, S., 2017. Recent advances in smart biotechnology: hydrogels and nanocarriers for tailored bioactive molecules depot. Adv. Colloid Interface Sci. 249, 163–180.
Morris, K.F., Johnson Jr., C.S., 1993. Resolution of discrete and continuous molecular size distributions by means of diffusion-ordered 2D NMR spectroscopy. J. Am. Chem. Soc. 115 (10), 4291–4299.
Pelta, M.D., Morris, G.A., Stchendroff, M.J., Hammond, S.J., 2002. A one-shot sequence for high-resolution diffusion-ordered spectroscopy. Magn. Reson. Chem. 40, S147–S152.
dos Santos, S., Medronho, B., dos Santos, T., Antunes, F.E., 2013. Amphiphilic molecules in drug delivery systems. Drug Delivery Systems – Advanced Technologies Potentially Applicable in Personalized Treatment. Springer.
Sehgal, P., Sharma, M., Wimmer, R., Larsen, K.L., Otzen, D.E., 2006. Interactions between anionic mixed micelles and α-cyclodextrin and their inclusion complexes: conductivity, NMR and fluorescence study. Colloid Polym. Sci. 284, 916–926.
Szejtli, J., 1998. Introduction and general overview of cyclodextrin chemistry. Chem. Rev. 98, 1743–1754.
Tanner, J.E., 1970. Use of the stimulated echo in NMR diffusion studies. J. Chem. Phys. 52, 2523–2526.
Tewes, F., Brillault, J., Couet, W., Olivier, J.-C., 2008. Formulation of rifampicin-cyclodextrin complexes for lung nebulization. J. Control. Release 129 (2), 93–99.
Thi, T.H.H., Azaroual, N., Flament, M.-P., 2009. Characterization and in vitro evaluation of the formoterol/cyclodextrin complex for pulmonary administration by nebulization. Eur. J. Pharm. Biopharm. 72 (1), 214–218.
Valente, A.J., Söderman, O., 2014. The formation of host-guest complexes between surfactants and cyclodextrins. Adv. Colloid Interface Sci. 205, 156–176.
Woessner, D.E., 2001. NMR relaxation of spin-3/2 nuclei: Effects of structure, order, and dynamics in aqueous heterogeneous systems. Concepts Magn. Reson. 13, 294–325.
Yan, Y., Jiang, L., Huang, J., 2011. Unveil the potential function of CD in surfactant systems. PCCP 13, 9074–9082.